ATMOSPHERIC CORROSION OF MAGNESIUM ALLOYS AZ31 AND AZ61 UNDER CONTINUOUS CONDENSATION CONDITIONS

Sebastián Feliu (Jr)[a] , C. Maffiotte[b], Juan Carlos Galván[a], Violeta Barranco[a,c].

[a]Centro Nacional de Investigaciones Metalúrgicas CSIC, Avda. Gregorio del Amo 8, 28040 Madrid, Spain, (e-mail: sfeliu@cenim.csic.es), (e-mail: jcgalvan@cenim.csic.es)

[b]CIEMAT. FNL (edificio 2), Avda. Complutense, 22, 28040 Madrid, Spain (e-mail: cesar.maffiotte@ciemat.es)

[c]Instituto de Ciencias de Materiales de Madrid, ICMM, Consejo Superior de Investigaciones Científicas, CSIC, Sor Juana Inés de la Cruz, 3, Cantoblanco, 28049, Madrid, Spain

Corresponding author: Tel.:+34 91 5538900. Fax.: +34 91 5347425. Email address: sfeliu@cenim.csic.es

Abstract

This paper studies the corrosion rate of magnesium alloys AZ31 and AZ61 exposed in humid air under continuous condensation conditions. The approximately parabolic shape of the corrosion progress curves suggests that the process is controlled by factors related with the corrosion product layer growing on the metallic surface. Complementary EIS measurements provide evidence of the restriction of surface activity by the accumulation of corrosion products. According to gravimetric results there is an initial period in which only a small part of the corroded metal is incorporated in the corrosion product layer, but after longer testing times the proportion of metal that comes to form part of this layer tends to increase very significantly.

Keywords: A. Magnesium alloys; B. EIS, XPS, SEM, weight loss; C. Atmospheric corrosion.

Introduction

The low density and appreciable mechanical strength of magnesium alloys makes them especially attractive for a wide range of practical applications, typically in the aerospace, automotive and electronics industries [1]. However, magnesium is a thermodynamically active metal, and consequently its corrosion behaviour is often a concern. It should be borne in mind that magnesium and its alloys tend to react with oxygen in the air and many aqueous media, when the protection afforded by the thin passivating film spontaneously formed on the surface of the metal fails for some reason.

It is always interesting to delve into knowledge of the corrosion behaviour of these materials in the various media and conditions in which they may be exposed [1-8]. The literature contains many such studies, often based on analysis of the results obtained using habitual laboratory techniques. In this respect, attention is drawn to those studies involving the immersion of specimens in NaCl solutions [9-17] which are particularly aggressive due to the presence of chloride ions. One benefit of immersion studies in saline solutions is that they facilitate the application of electrochemical techniques, which expand on the information supplied by gravimetric determinations. In fact, our understanding of the corrosion of magnesium alloys is largely based on immersion test studies.

Another type of test is that involving the exposure of specimens to the action of natural or artificial atmospheres, the latter in testing cabinets, and under controlled operative conditions representative of the multifarious circumstances of real-life exposure.

Such tests typically include high atmospheric humidity conditions [18-27], where the corrosion process in the humid atmosphere may be accelerated by the presence of pollutant gases or salts, as in the cases of spraying with saline solution or prior contamination of the metallic surface with NaCl [6,18,19,25,26]. To make the most of

the information provided by these tests, a knowledge is required of the phenomena and the mechanisms that control the corrosion process in each case.

This paper studies the corrosion rate of magnesium alloys exposed in humid air under continuous condensation conditions. There is relatively little information on the behaviour of these alloys under continuous condensation conditions in the absence of any type of contamination. In the present research the permanent presence of a condensed water layer in a process of constant renewal on the metallic surface offers conditions of special aggressivity.

For the performance of this research we have selected the magnesium alloys AZ31 and AZ61, with close to 3% and 6% Al, respectively. The microstructure of the first alloy is formed practically by an α-matrix with the aluminium in solid solution, while in the microstructure of the second alloy a large part of the aluminium has precipitated in the form of β-phase, with the possibility of galvanic coupling between the nobler β-phase and the magnesium alloy matrix, with the corresponding effect on corrosion [9,13]. With these alloys the research seeks to cover different possibilities in terms of the effect of the aluminium alloying element or the microstructure on the attack. Although it is not common to use AZ31 and AZ61 alloys in constant humidity condensation conditions, this is a matter of theoretic and practical interest since it adds to the information available on the behaviour of magnesium alloys in a variety of experimental circumstances and possible corrosion processes. In particular, it is of interest to know how the corrosion product layer formed on the metallic surface evolves and its relationship with the corrosion process kinetics.

Experimental

Materials

The chemical composition of the tested AZ61 and AZ31 magnesium alloys is given in Table 1. These alloys were fabricated in wrought condition and supplied in plates of 3 mm thickness by Magnesium Elecktron Ltd.

Surface conditions

The research also considers the possible effect on corrosion performance of a change in surface conditions of the tested specimens. Thus, the research includes specimens with the original (as-received) surface and others that have been mechanically polished prior to being subjected to the humidity condensation test.

Corrosion testing

Corrosion tests were performed in a continuous condensation cabinet, QCT Model ADO, and carried out according to International Standard ISO 6270-1:1998(E). Continuous condensation (CC) occurs on the metal surface at about 23ºC. The CC test provides an indication of the performance likely to be obtained in severe exposure conditions.

Gravimetric determinations

Gravimetric monitoring of the corrosion process has been carried out by exposing specimens to the CC test for 1, 7, 15, 30, 45 and 60 days. Practical considerations have limited to three the number of replicate specimens of each kind exposed for each exposure time. All the specimens have shown weight gains due to the predominance of corrosion products that remain in place over those that are eliminated from the tested surface. The amount of metal corroded has been obtained by weighing what is left after the removal of all adhered corrosion products by pickling in chromic acid. Weight losses were obtained by weighing the specimens to a precision of 0.001 mg .

EIS measurements

Electrochemical impedance spectroscopy (EIS) measurements have attempted to complement the information provided by gravimetric measurements of the specimens subjected to the CC test. For this purpose, the specimen was removed from the exposure cabinet after some testing time and taken to a conventional three-electrode cell, consisting of a reference electrode, counter electrode, and the corroded specimen as the working electrode. A 0.6M NaCl solution was used as electrolyte. Impedance spectra were obtained at the corrosion potential with an applied AC signal of 10 mV over the frequency range from 1 mHz to 100 KHz.

Metallography

The specimens were examined by scanning electron microscopy. The equipment used was a JEOL JXA 840A unit operating with Rontec EDR288 software for EDX spectra acquisition and image digitalisation.

Surface roughness measurements and AFM characterisation

The surface roughness was measured using an atomic-force microscope (AFM). The roughness value is expressed by the root mean square (RNS) value in nanometres, AFM images have also been obtained of the surface of the specimens in original (as-received) and polished conditions.

XPS analysis

Photoelectron spectra were acquired with a Fisons MT500 spectrometer equipped with a hemispherical electron analyser and a non-monochromatic magnesium Ka X-ray source operated at 300 W. Spectra were collected for 20-90 min, depending on the peak intensities, at a pass energy of 20 eV, which is typical of high-resolution conditions. It was possible to determine accurate binding energies by referencing to the adventitious C1s peak at 285.0 eV. Atomic ratios were computed from peak intensity ratios and reported atomic sensitivity factors [28]. The energy resolution is about 0.8 eV.

Results and discussion

An interesting point in this research is to elucidate the dependence of the corrosion rate on time. For gravimetric monitoring of the corrosion process, specimens have been exposed in triplicate in the condensation cabinet for time periods of up to 60 days. In addition to the corroded metal weight (C), these tests have yielded information on the weight gain (ΔW) of the specimens during the test and the weight (P) of the corrosion product layer formed on the metallic surface. A major difficulty when interpreting the values of C, ΔW and P is the large scatter of the gravimetric measurements, which can differ notably from specimen to specimen for each testing time (error bars in Fig. 1). In spite of this, the data in Fig.1 shows a clear tendency for corrosion to increase with time up to 30 days of exposure. This tendency is much less evident between 30 and 60

days of testing, and within the scatter of the results it is even doubtful whether corrosion continues to progress or has practically halted.

The great dispersion in repeated experiments suggests that the growth characteristics of the corrosion products layer are extraordinarily sensitive to fortuitous and minute variations in the formation process of this layer. In an attempt to reduce the dispersion of gravimetric data, another series of tests has been performed using the same specimens for all the test duration. In this case the periodic determinations of weight variation have been carried out by temporarily withdrawing the specimens from the humidity cabinet, allowing them to dry, weighing them, and then returning them to the cabinet to continue testing up to the scheduled time (60 days). In these determinations the gradual increase in the weight of the specimens principally reflects the progressive accumulation of corrosion products on their surface.

The ΔW vs. time curves in Fig. 2 show a deceleration of the corrosion process. The corrosion rate is highest at the start and subsequently declines probably due to the accumulation of protective corrosion products on the metal surface. Fig. 3, for the same series of tests as in Fig. 1, gives an idea of the increasing build-up of corrosion products with time.

The literature mentions the formation of coarse corrosion product layers on Mg and its alloys immersed in saline solution, whose growth barely affects the corrosion rate as a result of their high porosity [8,15,16]. In this investigation, the different behaviour of the specimens subjected to the CC test may be because of the lower porosity and greater protective capacity of the corrosion product layers formed on them. The electrochemical results presented in Fig. 4 are in line with this idea. This figure compares the impedance diagrams obtained after different immersion times in 0.6 M NaCl solution, for specimens directly immersed in this solution and specimens previously been exposed to the CC test for 30 days. In the latter case the corrosion product layer formed in the CC test allowed these specimens to show considerably higher impedance values in the first hours of immersion in the saline solution compared to those obtained without prior exposure. It is interesting to note that the effect of the corrosion product layer in the impedance values (diagrams in the second column of Fig. 4) disappears completely after 7 days of contact of the specimen with the aggressive saline solution.

The high Rt values per area unit (Table 2) suggest the existence of a very small fraction of free surface area on the specimens previously exposed to the CC test, possibly due to the low porosity of the corrosion product layer. In the same line, the capacitance values associated with this loop for these specimens are vastly smaller (of the order of 10^{-8} F/cm^2) than those determined for the specimens immersed directly in the saline solution without prior exposure to the CC test (which yield values of the order of 10^{-6} F/cm^2). All of these results, deduced from the impedance measurements, suggest the formation of much more compact layers in the CC test than in simple immersion.

Corrosiveness of the CC test

Table 3, prepared with data from the literature, compares the corrosiveness of the CC test used in the present work with that of other tests considered in different researches on the atmospheric corrosion of magnesium and its alloys. From the values shown in the last two rows of this table it is deduced that the corrosiveness of the CC test is much greater than that of other tests in atmospheres with high humidity levels that do not reach saturation (see start of table). However, the corrosiveness of the CC test is a little lower than that of tests which combine humid atmospheres and contamination of the metallic surface with NaCl, and notably lower than that of the salt spray test.

In humid atmospheres, in the presence of ambient concentrations of CO_2, all the metal suffers general corrosion and a thick corrosion product layer covers the specimen [18]. Two cathodic reactions are possible in principle: oxygen reduction and water reduction, although in many cases the latter:

$$H_2O + 2\ e^- \Rightarrow H_2\ (g) + 2\ OH^-$$

seems to be the only one of importance for magnesium corrosion [1, 8].

At the same time, the anodic reaction

$$Mg \Rightarrow Mg^{2+} + 2\ e^-$$

takes place and gives rise to the formation of brucite, $Mg(OH)_2$, which, at the CO_2 level found in the ordinary atmosphere, reacts with CO_2 to form magnesium hydroxide carbonates.

After some time a thick carbonate-containing corrosion product layer is formed. This layer may slow down the corrosion process by physically blocking active sites on the metal surface. It may also reduce the rate at which reactant species are transported through the corrosion product layer by reducing the section of the microchannels and/or increasing their length. In particular, an increase in the length of the diffusion paths with time could theoretically justify a parabolic rate law.

After an initial stage lasting a few days the specimen corrosion rate decelerates with testing time, which in the plot of Fig. 2 is translated into approximately parabolic curves, or into approximately straight sections when the abscissa is given in a $t^{1/2}$ scale (inset figure in the plot). Such behaviour suggests an effect of the corrosion product layer thickness on the kinetics of the process. This contrasts with published results on chloride induced atmospheric corrosion in humid air [8,16] and corrosion in saline solutions [25,26], which show a tendency for mass losses to increase linearly with time, possibly because in such cases the thickness of the highly porous layer does not control the corrosion rate. A complete understanding of the kinetics of the corrosion process in magnesium alloys exposed to the CC test does not seem possible with only gravimetric data. An explanation of how diffusion through the corrosion product layer could become the corrosion rate-determining step is suggested below.

Morphology and constitution of the corrosion product layer

Fig. 5 shows a SEM micrograph representative of the surface morphology of the corrosion products formed on the AZ61 and AZ31 alloys. Attention is drawn to the presence of a large number of needle-like clusters oriented nearly perpendicular to the specimen surface. Similar morphologies can be found in several studies on the corrosion of Mg and its alloys in immersion tests [30-32]. As can be seen, the structure is highly porous, which should allow diffusion through it.

The cross-section of this corrosion product layer in Fig. 6 shows important changes in its structure towards the metallic substrate. The needle-like crystallisations become less abundant and practically disappear in the final third of the corrosion product layer. The portion of the layer closest to the metallic surface is much more uniform and compact than near its outer surface, so it seems likely to play an important role in the kinetics of the corrosion process. Its evolution with time may have influenced the approximately parabolic plot of the graphs in Fig. 2.

Table 4 shows the element composition on the surface of the AZ61 and AZ31 alloys after exposure to the CC test. The O/(Mg+Al) atomic ratios obtained with the AZ61 alloy reach values of close to 2, which tends to suggest that the specimen surface is essentially covered by an oxide layer of $Mg(OH)_2$. On the exposed surface of the AZ31 alloy, this ratio reaches values of close to 3; an increase that can presumably be accounted for by the formation of magnesium carbonate on the exposed surface.

Additional information from gravimetric data

Apart from the kinetic aspects considered above, it is of interest to analyse the information derived from the relationships established between the parameters C, ΔW and P defined above. This information can provide insight into some of the characteristics of the corrosion products layer during the different stages of their formation and growth.

C/P ratio. Obviously, the relationship between weight of corroded metal and the weight of the corrosion product layer will be very high when only a small part of the corroded metal precipitates on the specimen. The lowest value will correspond to the extreme case in which all the corroded metal comes to form part of the corrosion product layer. According to the literature, in atmospheres with high humidity levels and in the presence of ambient levels of CO_2, the corrosion of magnesium and its alloys gives rise to the formation of hydrated magnesium hydroxy carbonate with compositions close to hydromagnesite $Mg_5(CO_3)_4(OH)_2.4H_2O$ [25]. Accepting the formation of this type of compounds, the lowest possible C/P ratio value (equivalent to the fraction of Mg in the corrosion products) would be approximately 0.26.

The high C/P ratio values in Fig. 7 show that at the start of the test only a small portion of the corroded metal has been used in the formation of the corrosion product layer. A clear difference is seen between the specimens whose surface had been mechanically polished prior to the test and those tested with the original surface, which present the lowest C/P ratios. As exposure time increases, the C/P ratio quickly decreases and the values for the different alloys and surface conditions tend to equalise around a value of $\sim$ 0.25-0.30, a sign that practically all the corroded metal has come to form part of the corrosion product layer.

ΔW/P ratio. The maximum value reachable by this ratio (y-axis in Fig. 8) corresponds to the condition in which all the corroded metal is used in the formation of the corrosion product layer. Assuming that the Mg fraction in the corrosion product composition is 0.25-0.30, a maximum ΔW/P value of 0.70-0.75 is deduced. This value is reached after approximately 15 days of testing (Fig. 8). The ΔW/P values are exceptionally low in the first days of testing, especially in the case of the unpolished surfaces, which suggests greater difficulty for the nucleation and initial growth of the corrosion product layer on these surfaces.

C/ΔW ratio. Although it is not always exactly known how much of the corroded metal is represented in the measured specimen weight gain, the literature includes cases where the ΔW value is used to monitor the progress of corrosion. The ideal condition for the achievement of a proportionality between C and ΔW is that all the corroded metal should be incorporated in the layer of corrosion products. According to the values above, for this to happen the C/ΔW ratio should reach a maximum value of 0.33-0.43. The polished specimens show C/ΔW values close to this value after about 7-15 days of testing (Fig. 9), while the specimens with the original surface have C/ΔW values well above 0.33-0.43 at the start of the test, and tend towards this limit much more slowly (Fig. 9).

Effect of alloy type and surface conditions

It should be noted that the surface conditions have a certain effect on the behaviour of the specimens (Figs. 1, 2, 7-9). This is very clearly seen in Fig. 2, where the points corresponding to the original surface condition are always found above those corresponding to the polished surface condition, for both alloys and testing times. This appears to suggest a greater compactness of the corrosion product layer formed on the polished surface than that formed on the original surface, perhaps because the presence of oxides and some other possible species present in the rolling skin from the fabrication process perturbs the normal growth of the corrosion product layer on the as-received surface.

Conclusions

The performance of AZ31 and AZ61 magnesium alloys has been studied in a high humidity atmosphere under continuous condensation (CC) conditions. One of the purposes of the work was to study experimental conditions without the influence of chloride ions which are often present in research on atmospheric corrosion in the literature. The high scatter of gravimetric results for the specimens subjected to the CC test suggests an extraordinary sensitivity of the corrosion product layer's growth characteristics to fortuitous minute variations in the process of their formation.

In the series of tests with the AZ31 and AZ61 specimens the rate of attack tends to diminish as a function of time suggesting some protective action of the growing corrosion product layer. This behaviour differs from the approximately linear rate laws in published work on the atmospheric corrosion of magnesium and its alloys in the presence of chlorides, and is more in concordance with the behaviour expected of a layer whose thickness controls the corrosion rate.

Analysis of the set of gravimetric data has revealed a first period during which only a small part of the corroded metal participates in the formation of the corrosion product layer on the metal surface. The proportion of metal that forms this layer increases with exposure time to the point that all the corroded metal is incorporated. The time taken to reach this situation depends significantly on the initial conditions of the exposed metallic surface.

The EIS technique was also employed in order to better characterise the protective action of the corrosion product layers on the tested magnesium alloys. These measurements show a strong restrictive effect on surface activity in the specimens upon which coarse corrosion product layers have built up in exposure to the CC test.

Acknowledgment

We wish to express our gratitude to Prof. S. Feliu for several clarifying and stimulating discussions during the course of this work. Also, the authors gratefully acknowledge the financial support for this work from the Ministry of Science and Innovation of Spain (MAT 2009-13530)

References

1. G. Song, A. Atrens, Adv. Eng. Mater., 5 (2003) 837-858.

2. G. Song, A. Atrens, M. Dargusch, Corros. Sci., 41 (1999), 249-273.

3. M. Jönsson, D. Persson, G. Leygraf, Corros. Sci., 50 (2008) 1406-1413.

4. J.H. Nordlien, K. Nisancioglu, S. Ono, N. Masuko, J. Electrochem. Soc., 143 (1996), 2564-2572.

5. J.H. Nordlien, K. Nisancioglu, S. Ono, N. Masuko, J. Electrochem. Soc., 144 (1997) 461-466.

6. C. Fotea, J. Callaway, M. R. Alexander, Surf. Interface Anal., 38 (2006) 1363-1371.

7. M-C. Zhao, P. Schmutz, S. Brunner, M. Liu, G. Song, A. Atrens, Corros. Sci., 51 (2009) 1277-1292.

8. G. Baril, N. Pébère, Corros. Sci., 43 (2001), 471-484.

9. G. Song, A. Atrens, D. St. John, X. Wu, J. Nairn, Corros. Sci., 39 (1997) 1981-2004.

10. G. Song, A. Atrens, X. Wu, B. Zhang, Corros. Sci., 40 (1998) 1769-1791.

11. G. Song, A. Atrens, D. St. John, J. Nairn, Y. Li, Corros. Sci., 39 (1997) 855-875.

12. S. Mathieu, C. Rapin, J. Steinmetz, P. Steinmetz, Corros. Sci., 45 (2003) 2741-2755.

13. S. Mathieu, C. Rapin, J. Hazan, P. Steinmetz, Corros. Sci., 44 (2002) 2737-2756.

14. G.L. Makar, J. Kruger, J. Electrochem. Soc., 137 (1990) 414-421.

15. M. Santamaria, F. Di. Quarto, S. Zanna, P. Marcus, Electrochim. Acta, 53 (2007) 1314-1324.

16. A. Pardo, M.C. Merino, A.E. Coy, F. Viejo, R. Arrabal, S. Feliu Jr., Electrochim. Acta, 53 (2008) 7890-7902.

17. G. Galicia, N. Pébère, B. Tribollet, V. Vivier, Corros. Sci., 51 (2009) 1789-1794.

18. R. Lindström, J-E. Svensson, L-G. Johansson, J. Electrochim. Soc., 149 (2002) B103-B107.

19. R. Lindström, L-G. Johansson, J-E. Svensson, Materials and Corrosion, 54 (2003) 587-594.

20. R. Lindström, L-G. Johansson, G.E. Thompsson, P. Skeldon, J-E. Svensson, Corros. Sci., 46 (2004), 1141-1158.

21. S.J. Splinter, N.S. McIntyre, Surf. Sci., 314(1994) 157-171.

22. J. H. Nordlien, S. Ono, N. Masuko, K. Nisancioglu, Corros. Sci., 39 (1997) 1397-1414.

23. N.S. McIntyre, C. Chen, Corros. Sci. 40 (1998) 1697-1709.

24. M. Jönsson, D. Persson, R. Gubner, J. Electrochem. Soc., 1954 (2007), C684-C691.

25. M. Jönsson, D. Persson, D. Thierry, Corros. Sci., 49 (2007), 1540-1558.

26. G. Ballerini, U. Bardi, R. Bignucolo, G. Ceraolo, Corros. Sci., 47 (2005) 2173-2184.

27. R. Arrabal, A. Pardo, M.C. Merino, S. Merino, M. Mohedano, P. Casajus, Materials and Corrosion, 61 (2010) 1-9.

28. S. Feliu Jr., A. Pardo, M.C. Merino, A.E. Coy, F. Viejo, R. Arrabal, Appl. Sur. Sci., 255 (2009) 4102-4108.

29. C.D. Wagner, L.E. Davis, M.V. Zeller, J.A. Taylor, R.H. Raymond, L. Gate, Surf. Interface Anal., 3 (1981) 211-225.

30. C.B. Baliga, P. Tsakiropoulos, Mater. Sci. Technol., 9 (1993) 513-519.

31. X. Guo, J. Chang, S. He, W. Ding, X. Wang, Electrochim. Acta, 52 (2007) 2570-2579.

32. J. Chang, X. Guo, S. He, P. Fu, L. Peng, W. Ding, Corros. Sci., 50 (2008) 166-177.

33. R. Ambat, N.N. Aung, W. Zhou, Corros. Sci., 314 (1994) 157-171.

34. S. Feliu Jr., M.C. Merino, R. Arrabal, A.E. Coy, E. Matyking, Surf. Interface Anal., 41 (2009) 143-150.

35. M. Liu, P.D. Uggowitzer, A.V. Nagasekhar, P. Schmutz, M. Easton, G. Song, A. Atrens, Corros. Sci., 51 (2009) 602-619.

TABLE 1. Chemical composition of the tested magnesium alloys.

Material	Al	Zn	Mn	Si	Cu	Fe	Ni	Ca	Zr	Others
AZ31	3.1	0.73	0.25	0.02	<0.001	0.005	<0.001	0.0014	<0.001	<0.30
AZ61	6.2	0.74	0,23	0.04	<0.001	0.004	<0.001	0.0013	<0.001	<0.30

TABLE 2. Rt values obtained after one hour in 0.6 M NaCl solution of specimens previously exposed to the CC test for different times.

ALLOY	Rt VALUES ($\Omega.cm^2$)			
	Exposure time to the CC test			
	1 day	15 days	30 days	40 days
AZ31	1×10^3	1×10	1×10	1×10
AZ61	3×10^3	2×10^4	3×10^4	---

TABLE 3. Literature data. Parentheses enclose approximate corrosion values calculated from published weight gain determinations.

Ref.	Test conditions	Material	Corrosion (mg/cm^2)		
			7 days	15 days	30 days
19	95% RH, 22ºC	AZ91D	--	--	~0
20	95% RH, 22ºC	Mg	--	--	0.01
28	98% RH, 50ºC	Mg	(0.06)	(0.12)	(0.17)
28	98% RH, 50ºC	AZ31	(0.03)	(0.08)	(0.12)
28	98% RH, 50ºC	AZ80	(0.008)	(0.034)	(0.057)
28	98% RH, 50ºC	AZ91D	(0.014)	(0.053)	(0.072)
19	95% RH, 22ºC 15 µg/cm^2 NaCl added	AZ91D	---	---	(0.10)
19	95% RH, 22ºC 36 µg/cm^2 NaCl added	AZ91D	---	---	(0.17)
19	95% RH, 22ºC 74 µg/cm^2 NaCl added	AZ91D	---	---	(0.23)
25	95% RH, 25ºC 70 µg/cm^2 NaCl added	AZ91D	0.15	0.30	0.47
18	95% RH, 22ºC 70 µg/cm^2 NaCl added	AM20	(0.33)	(0.60)	(0.73)
18	95% RH, 22ºC 70 µg/cm^2 NaCl added	AM60	(0.26)	(0.36)	(0.50)
18	95% RH, 22ºC 70 µg/cm^2 NaCl added	AZ91D	(0.18)	(0.21)	(0.23)
26	Salt spray test 5 wt% NaCl, 35ºC	AZ91D	1.6	2.5	---
This work	Continuous condensation, 23º	AZ31	0.07	0.15	0.38
This work	Continuous condensation, 23º	AZ61	0.23	0.21	0.36

TABLE 4. Atomic composition obtained by XPS of the surface of AZ31 and AZ61 specimens after exposure to the humidity condensation test.

SAMPLE	%C	%O	%Mg	%Al	O/(Mg+Al)	Al/(Mg+Al)x100
AZ31	16	61	22	1	2.7	4
AZ61	16	56	24	4	2	14

Figure captions

Fig. 1. Corrosion loss as a function of exposure time.

Fig. 2. Specimen weight gain as a function of exposure time. The standard deviation of measurements is about 20%.

Fig. 3. Increase in weight of corrosion product layer as a function of exposure time.

Fig. 4. Comparison of impedance diagrams for specimen immersed in 0.6 M NaCl solution after 30 days of prior exposure to the CC test (right column) and without prior exposure (left column).

Fig. 5. Image of corrosion products formed on the specimen surface during exposure to the CC test.

Fig. 6. Cross-section of corrosion product layer between the metal substrate and the resin as mounting material. The crack in the corrosion products layer (near its junction with the metal surface) was caused during preparation of the specimen for microscopic examination.

Fig. 7. C/P ratio as a function of exposure time.

Fig. 8. ΔW/P ratio as a function of exposure time.

Fig. 9. C/ΔW ratio as a function of exposure time.

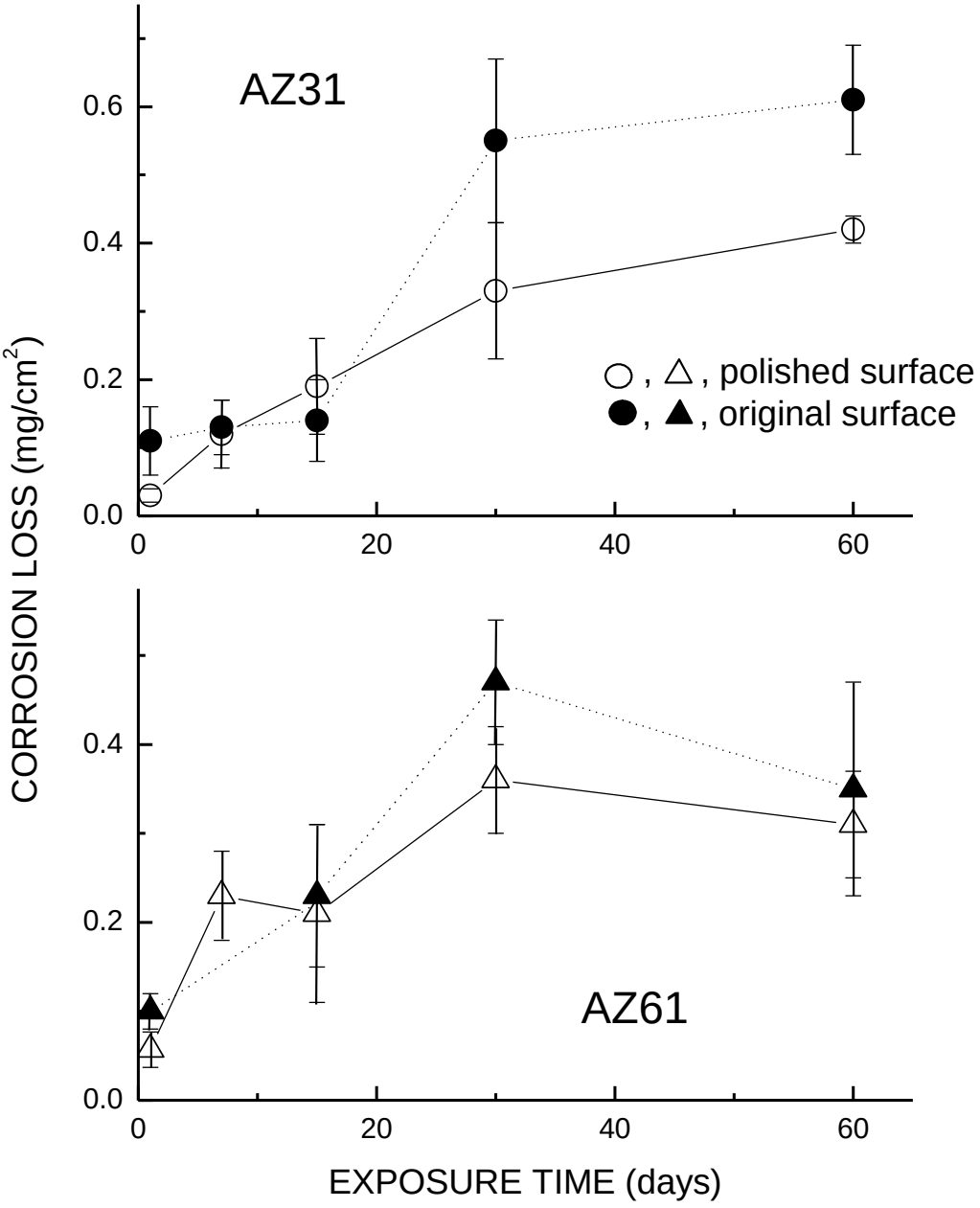
AZ31
AZ61
○ , △ , polished surface
● , ▲ , original surface
CORROSION LOSS (mg/cm²)
EXPOSURE TIME (days)
0.0
0.2
0.4
0.6
0
20
40
60

Fig 1.

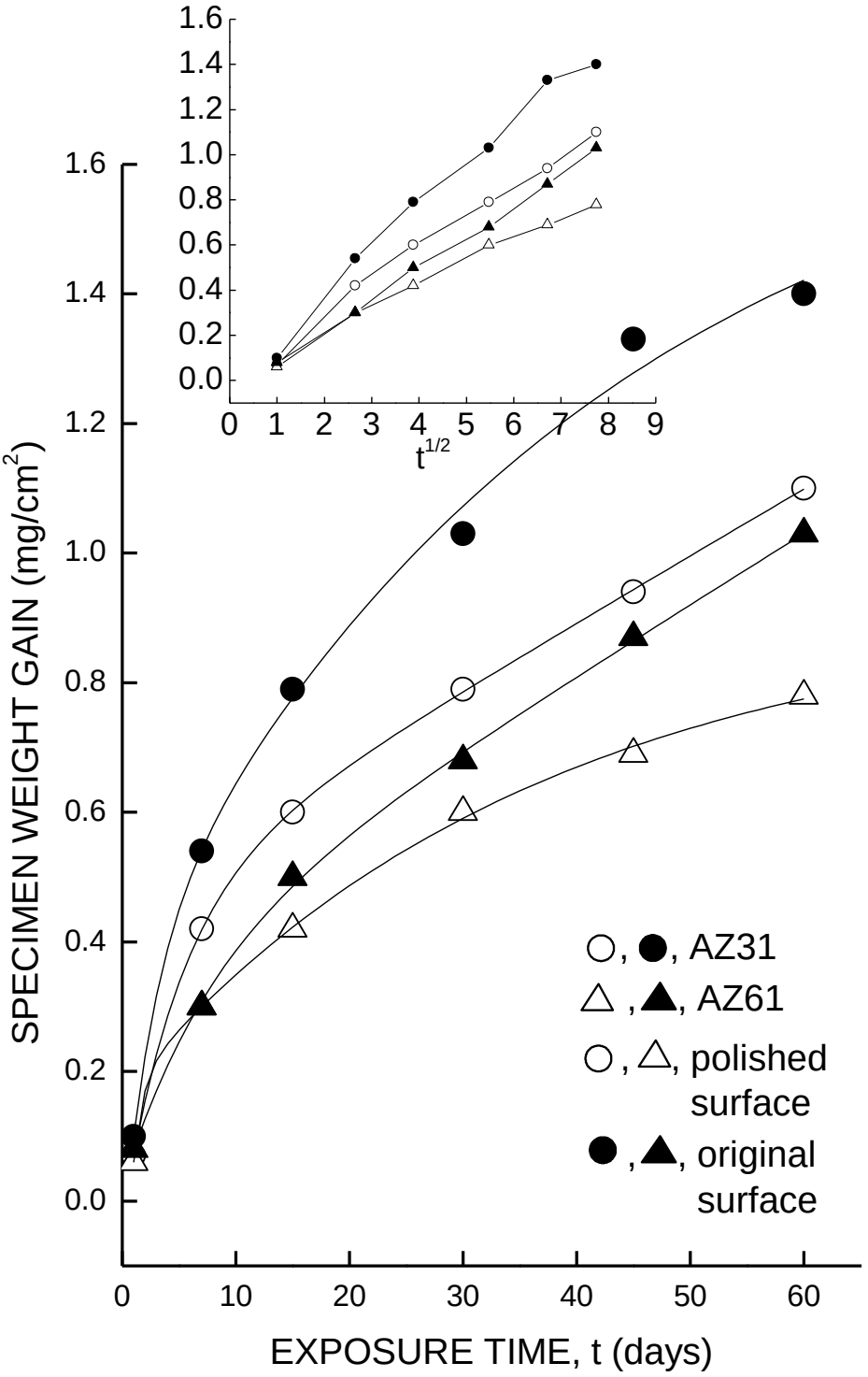
SPECIMEN WEIGHT GAIN (mg/cm^2)
EXPOSURE TIME, t (days)
$t^{1/2}$
○, ●, AZ31
△ ,▲, AZ61
○ , △, polished surface
● ,▲, original surface

Fig. 2

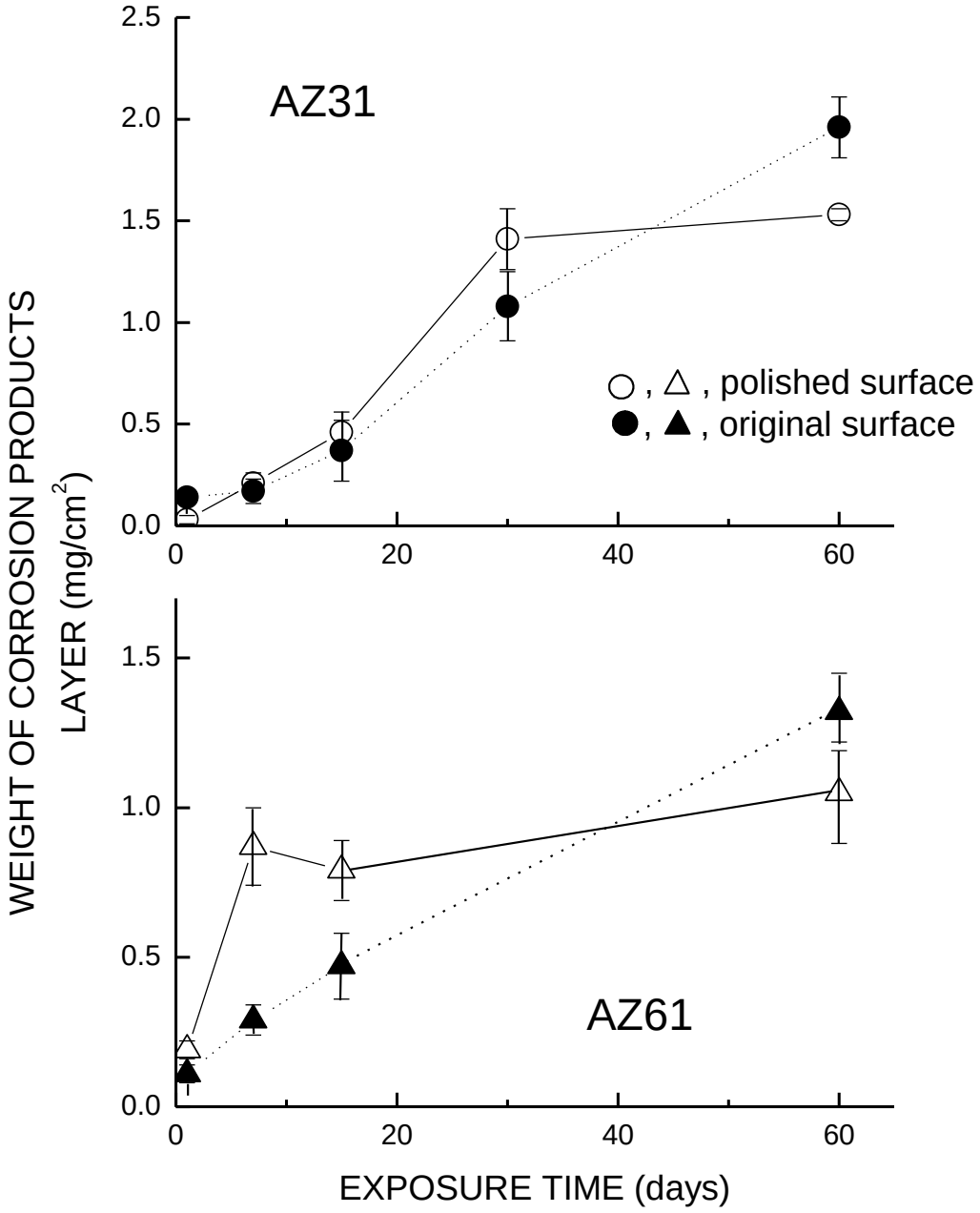
AZ31
AZ61
○ , △ , polished surface
● , ▲ , original surface
WEIGHT OF CORROSION PRODUCTS LAYER (mg/cm^2)
EXPOSURE TIME (days)
0.0
0.5
1.0
1.5
2.0
2.5
0
20
40
60

Fig. 3

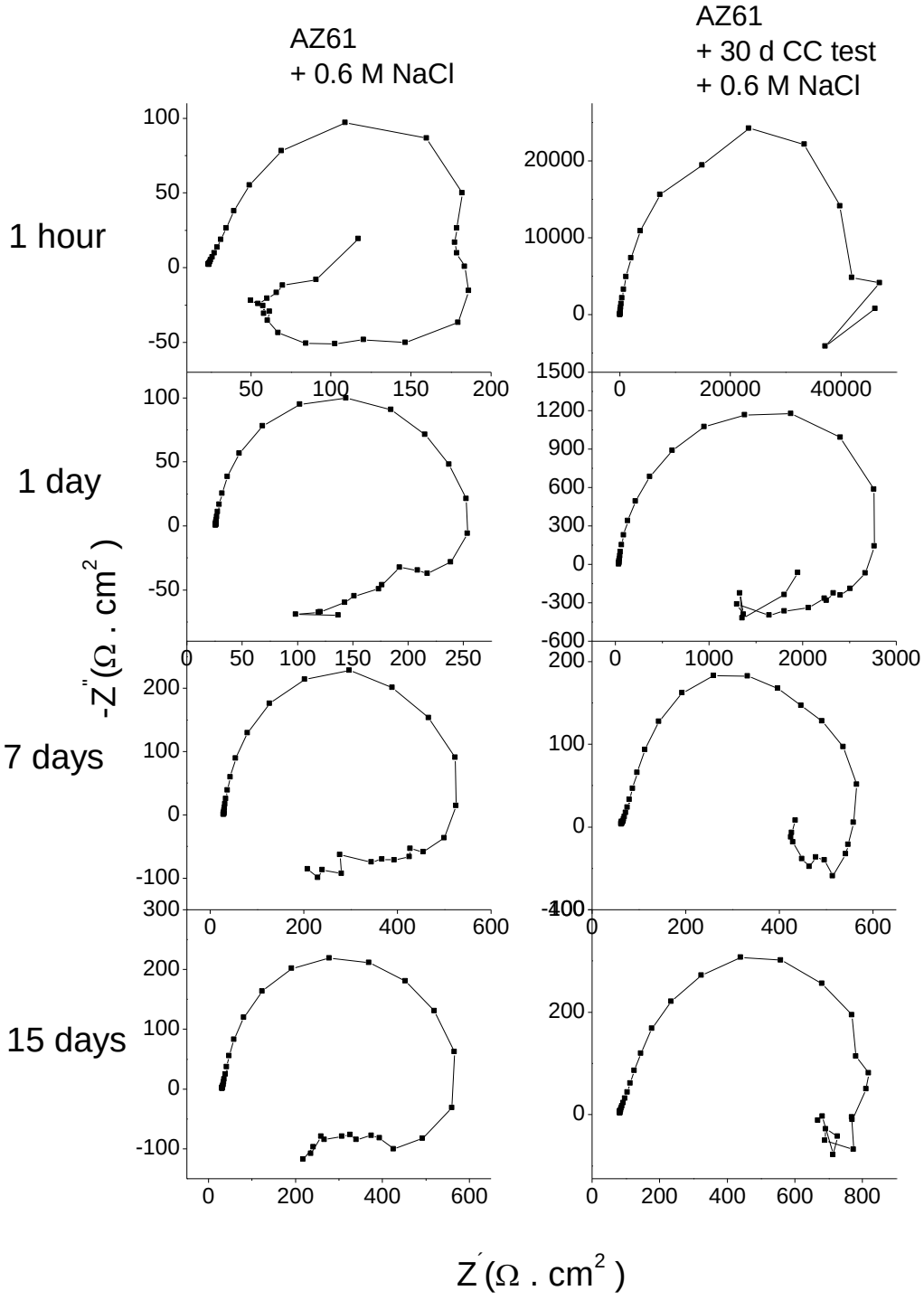
AZ61
+ 0.6 M NaCl
AZ61
+ 30 d CC test
+ 0.6 M NaCl
1 hour
1 day
7 days
15 days
-Z˝(Ω . cm²)
Z´(Ω . cm²)

Fig.4

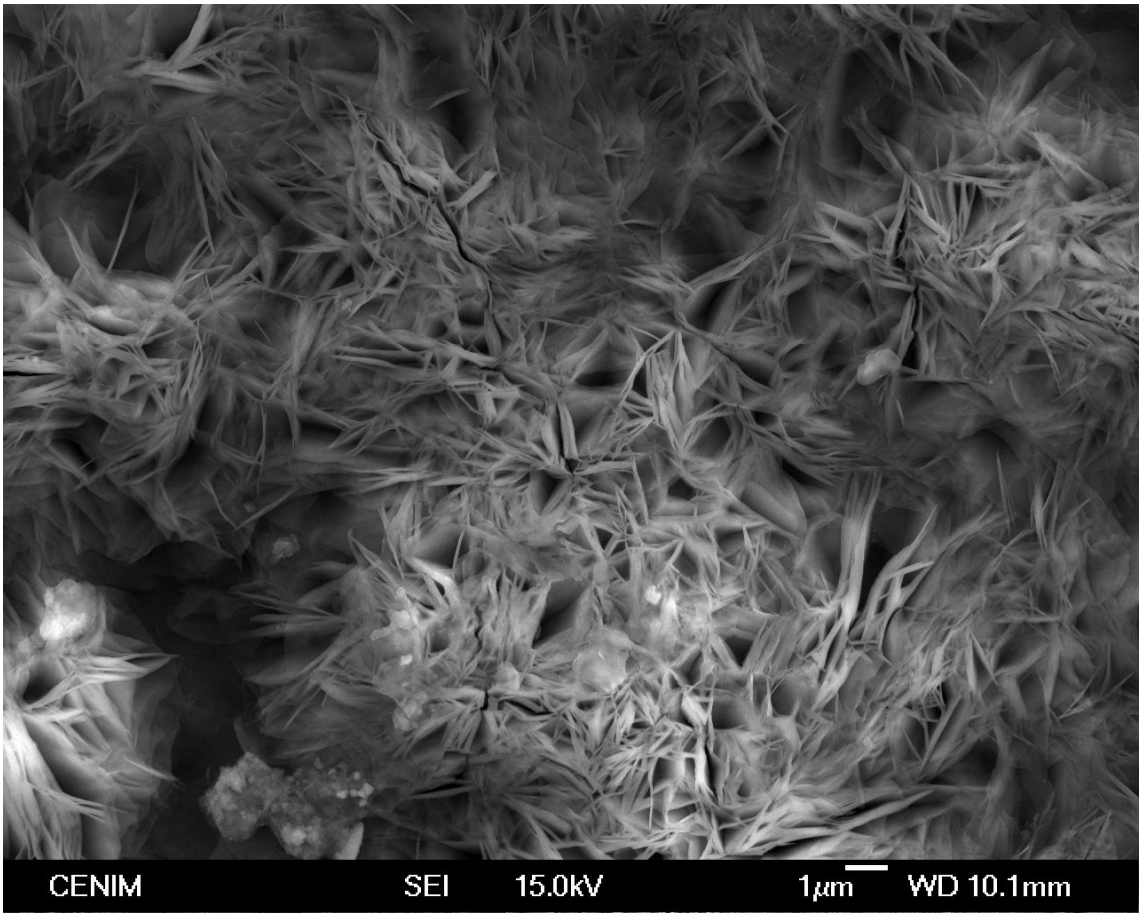

Fig.5

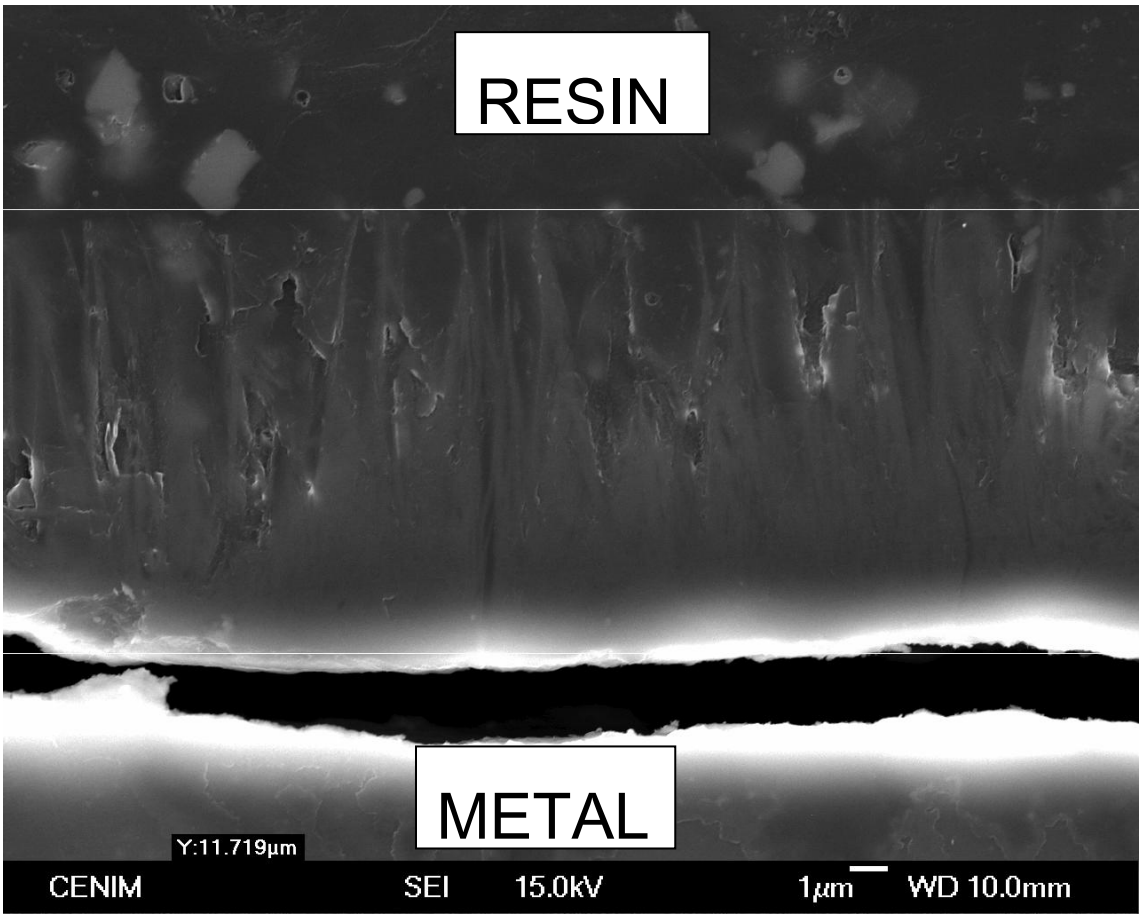

Fig 6.

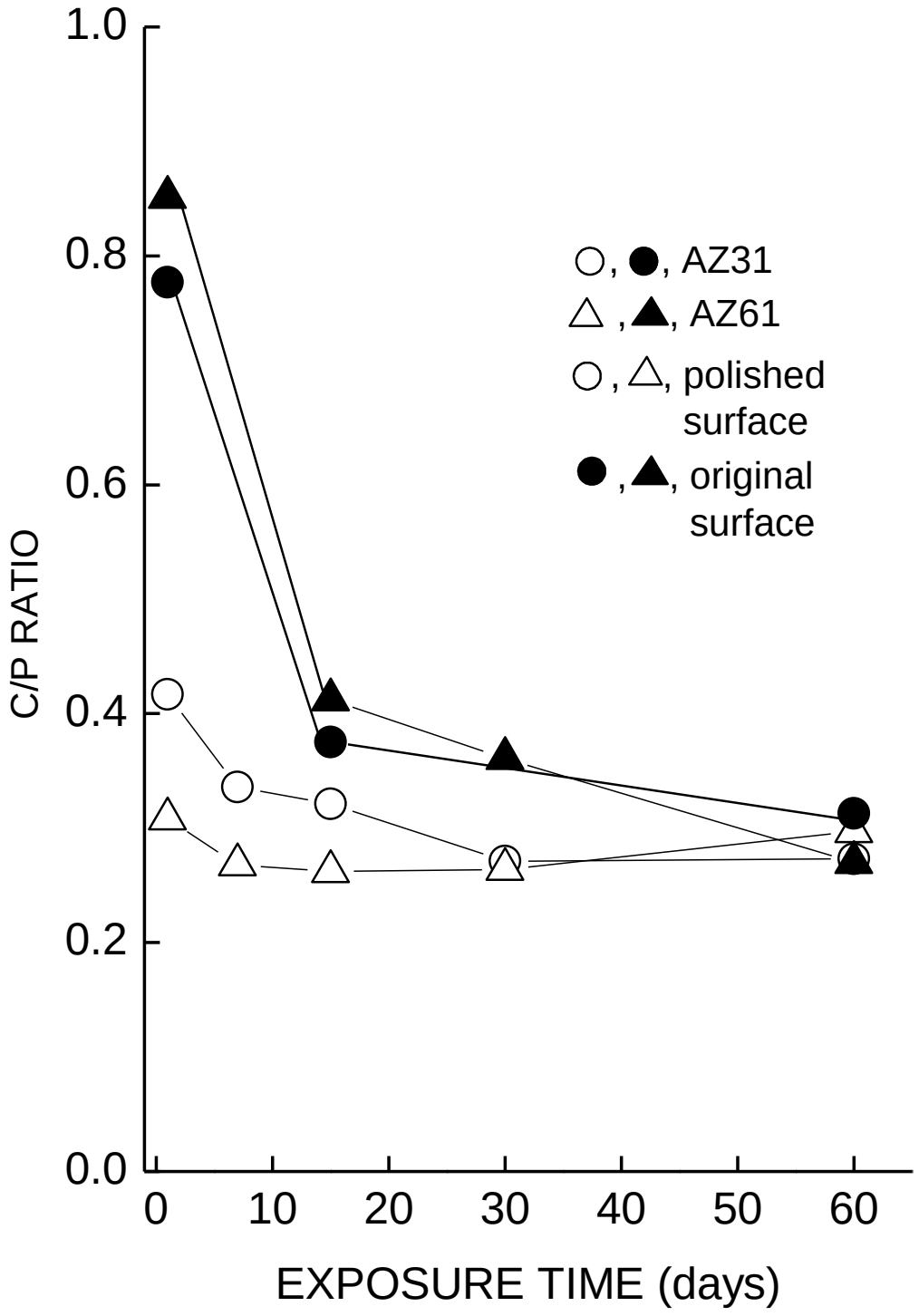
1.0
0.8
0.6
0.4
0.2
0.0
C/P RATIO
0
10
20
30
40
50
60
EXPOSURE TIME (days)
○, ●, AZ31
△ ,▲, AZ61
○ , △, polished surface
● ,▲, original surface

Fig. 7

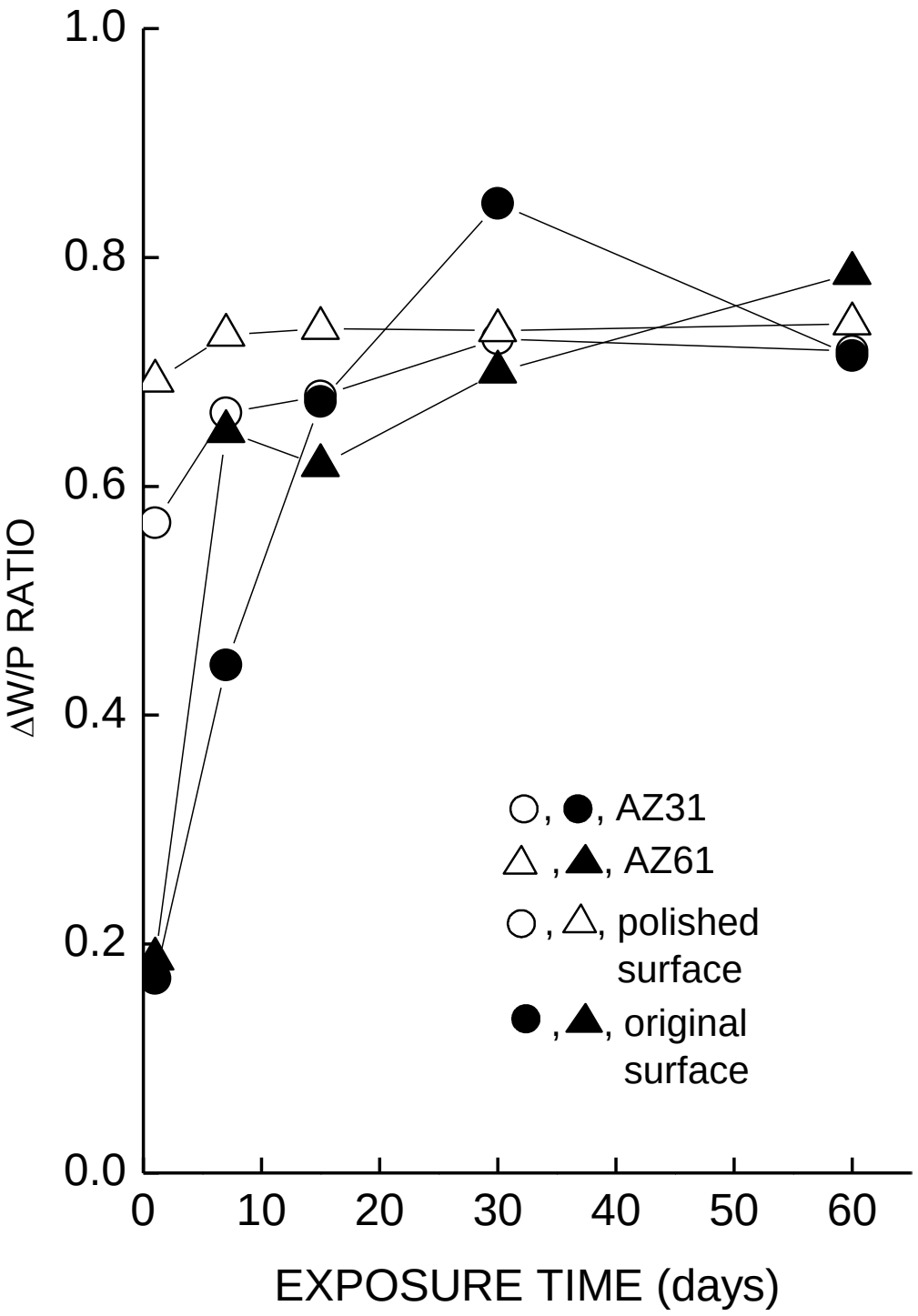
1.0
0.8
0.6
0.4
0.2
0.0
ΔW/P RATIO
0
10
20
30
40
50
60
EXPOSURE TIME (days)
○, ●, AZ31
△ ,▲, AZ61
○ , △, polished surface
● ,▲, original surface

Fig.8

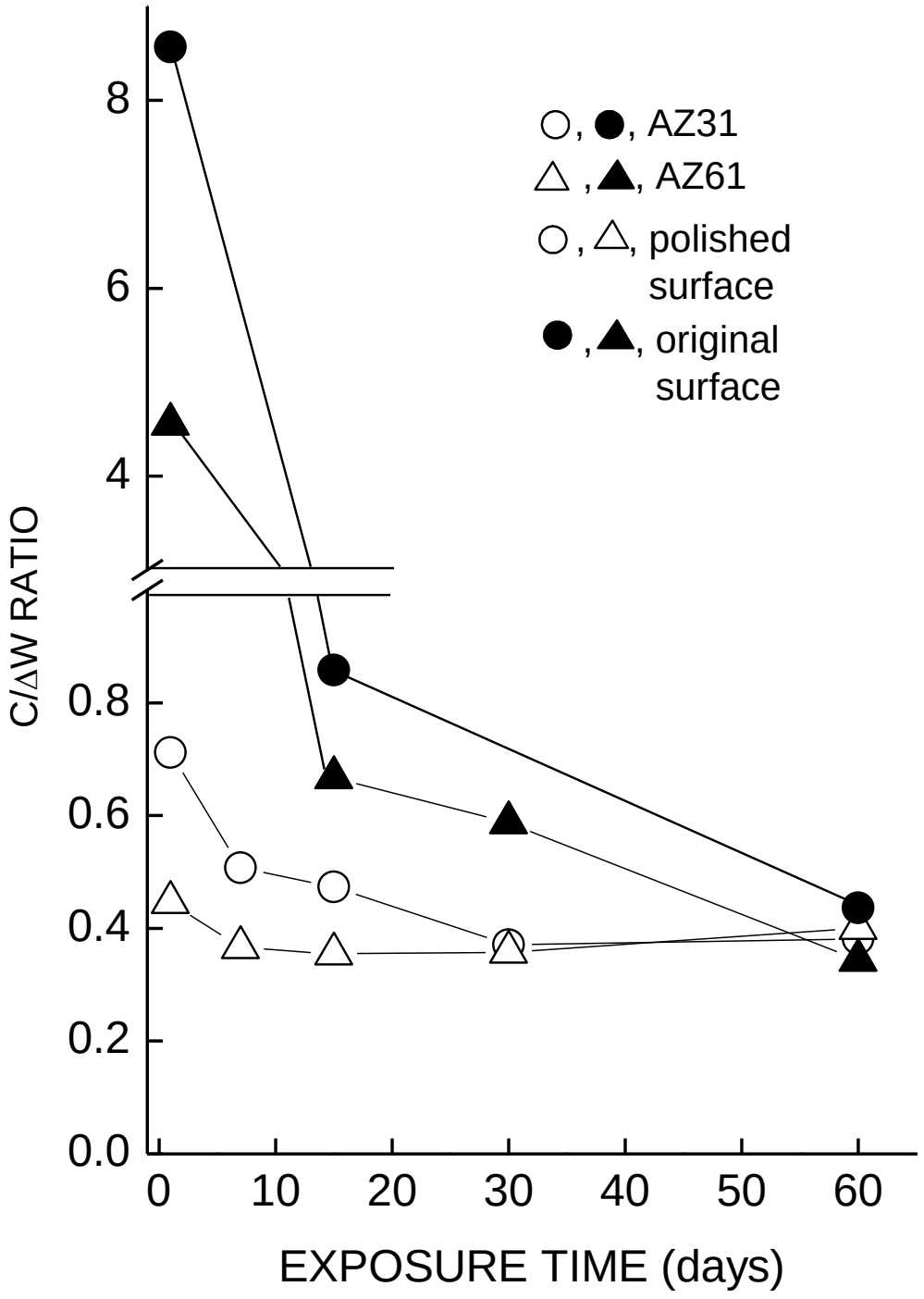
8
6
4
0.8
0.6
0.4
0.2
0.0
0
10
20
30
40
50
60
C/ΔW RATIO
EXPOSURE TIME (days)
○, ●, AZ31
△ ,▲, AZ61
○ , △, polished surface
● ,▲, original surface

Fig. 9